ENVIRONMENTAL EPIGENETICS

Environmental Epigenetics, 2023, **9(1)**, 1–15
DOI: https://doi.org/10.1093/eep/dvad003
Advance Access Publication 3 June 2023
Research Article

Transgenerational sperm DMRs escape DNA methylation erasure during embryonic development and epigenetic inheritance

Millissia Ben Maamar[1,3], Yue Wang[2], Eric E. Nilsson[1], Daniel Beck[1], Wei Yan[2] and Michael K. Skinner[1,*]

[1]Center for Reproductive Biology, School of Biological Sciences, Washington State University, Pullman, WA 99164, USA, [2]David Geffen School of Medicine at UCLA, The Lundquist Institute at Harbor-UCLA Medical Center, Torrance, CA 90502, USA
[3]Present address: TekTeam Medical Consulting, Palo Alto, CA 94303, USA
*Correspondence address. Center for Reproductive Biology, School of Biological Sciences, Washington State University, Pullman, WA 99164, USA. Tel: +509-335-1524; E-mail: skinner@wsu.edu

Abstract

Germline transmission of epigenetic information is a critical component of epigenetic inheritance. Previous studies have suggested that an erasure of DNA methylation is required to develop stem cells in the morula embryo. An exception involves imprinted genes that escape this DNA methylation erasure. Transgenerational differential DNA methylation regions (DMRs) have been speculated to be imprinted-like and escape this erasure. The current study was designed to assess if morula embryos escape the erasure of dichlorodiphenyltrichloroethane–induced transgenerational sperm DMR methylation. Observations demonstrate that the majority (98%) of transgenerational sperm DMR sites retain DNA methylation and are not erased, so appearing similar to imprinted-like sites. Interestingly, observations also demonstrate that the majority of low-density CpG genomic sites had a significant increase in DNA methylation in the morula embryo compared to sperm. This is in contrast to the previously observed DNA methylation erasure of higher-density CpG sites. The general erasure of DNA methylation during embryogenesis appears applicable to high-density DNA methylation sites (e.g. CpG islands) but neither to transgenerational DMR methylation sites nor to low-density CpG deserts, which constitute the vast majority of the genome's DNA methylation sites. The role of epigenetics during embryogenesis appears more dynamic than the simple erasure of DNA methylation.

Key words: epigenetics; DNA methylation; transgenerational; inheritance; embryo; morula; development; review

Introduction

Environmentally induced epigenetic transgenerational inheritance was originally observed with the use of the agricultural fungicide vinclozolin toxicant [1] and subsequently with stress [2] in rodents. Over the past decades, all organisms studied have been shown to display epigenetic transgenerational inheritance, and a large number of different toxicants [3], stress conditions [4, 5], nutrition abnormalities [6], and a variety of different environmental factors [3] have been shown to induce epigenetic transgenerational inheritance. In plants, worms, and flies, the altered phenotypes can be transmitted for hundreds of generations, while in rodents and humans, three to five generations have been examined [7]. The environmental exposures alter the epigenome of the germline (sperm and egg), which appears to impact the early embryo epigenetics and transcriptome to alter all derived somatic cells and induce transgenerational phenotypes [7]. This non-genetic form of inheritance is mediated through combined actions of a number of different epigenetic processes in the germline including DNA methylation, histone modifications, non-coding RNA, and chromatin structure [8, 9].

Following fertilization of the oocyte with the sperm, the zygote develops as a diploid cell in the first stage of embryonic development. Zygotic genome activation and epigenetic programming are involved in the initiation of embryonic development [10]. The zygote undergoes the first cleavage event to the two-cell embryo, and then, rapid mitotic divisions occur to develop the morula embryo, which contains the totipotent morula stem cells. These morula cells will initiate the eventual development into all somatic cell lineages in the organism. The morula then develops into the blastula that following implantation completes the subsequent stages of embryogenesis and cell development (Fig. 1A). The previous work by Monk *et al.* [11], using restriction enzyme analysis, and the recent studies reviewed by Reik and Surani [12], using bisulfite sequencing, have demonstrated a DNA methylation erasure during these early stages of embryo development from the zygote to the morula and subsequent early blastula stages.

Received 14 March 2023; **revised** 10 May 2023; **accepted** 1 June 2023

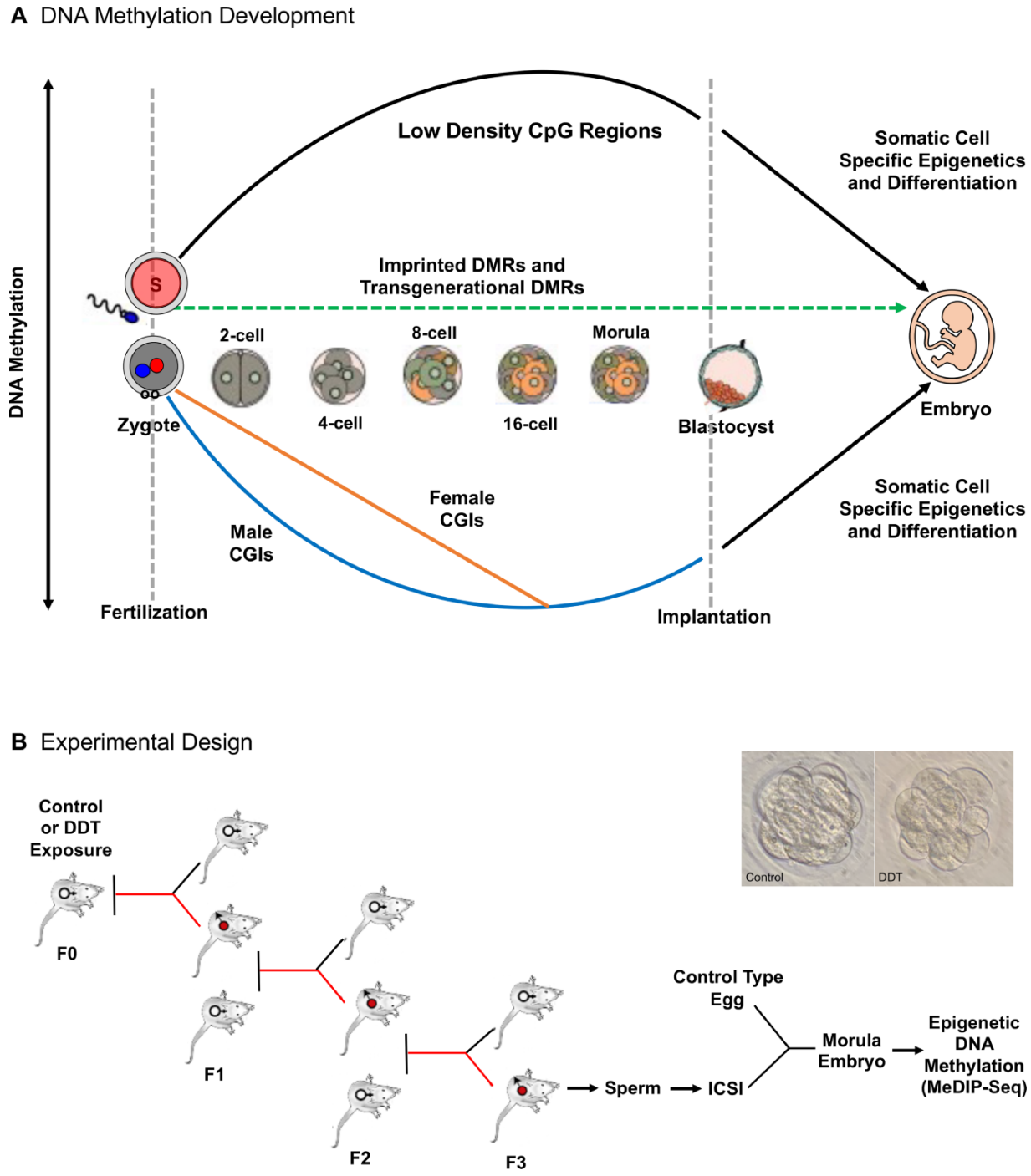

Figure 1: The sperm and morula embryo DNA methylation summary. **(A)** The schematic of DNA methylation following fertilization in early embryo development. **(B)** Experimental design and morula histology.

This is thought to allow an epigenetic reset of the embryo and facilitate the development of the pluripotent stem cells and subsequent development of the somatic cell populations [13]. Previous research into imprinted genes has demonstrated that these DNA methylation sites are protected from erasure to maintain DNA methylation during embryonic development, which has a critical functional role during embryogenesis and fetal development [14]. Therefore, the early embryo has dramatic epigenetic alterations involving DNA methylation erasure. Mechanisms exist, such as the presence of Kruppel-associated box domain zinc finger and the tripartite motif–containing protein 28 DNA-binding proteins [15–17], to protect critical epigenetic sites from DNA methylation erasure [18, 19]. Therefore, mechanisms exist to prevent the DNA methylation erasure.

Following the initial observations of environmentally induced epigenetic transgenerational inheritance, the suggestion was made that the transgenerational differential DNA methylation regions (DMRs) identified would be imprinted-like and maintain their methylation and allow DMR site protection from erasure [1, 20]. The current study used intracytoplasmic sperm injection (ICSI) of control and dichlorodiphenyltrichloroethane (DDT) lineage transgenerational (F3 generation) sperm to generate morula

stage embryos for the analysis of DNA methylation status of the DMR sites. Previously, a large number of different toxicants, such as the fungicide vinclozolin, plastic-derived compounds, the herbicide glyphosate, or jet fuel hydrocarbons, have been shown to promote similar transgenerational pathologies, but each has distinct transgenerational epigenetic alterations [1, 7, 21–28]. Therefore, the DDT impacts observed in the current study are anticipated to be similar to those of other environmental factors promoting epigenetic transgenerational inheritance. Observations of the current study demonstrate that a large number of the environmentally induced transgenerational DMR methylation sites appear to escape DNA methylation erasure. Therefore, environmentally induced transgenerational sperm epimutations appear to escape DNA methylation erasure to impact embryonic cell epigenetics and transcriptomes to then alter subsequent somatic cell epigenetics and phenotypes. Interestingly, an additional observation made in the current study was that lower-density CpG genomic sites were also found to escape DNA methylation erasure and generally have an increase in DNA methylation. Therefore, the reprogramming of the epigenome during early embryonic development appears dynamic, with both decreases and increases in DNA methylation (Fig. 1A).

Results

The experimental design involved a transient environmental exposure (i.e. DDT or a dimethyl sulfoxide vehicle control) of a gestating female outbred Sprague Dawley (SD) rat during embryonic Days 8–14 (i.e. gonadal sex determination period) followed by the subsequent breeding of the F1 and F2 generations to generate the F3 generation [29] (Fig. 1B), as described in the Methods. The exposure period corresponds to fetal gonadal sex determination when the male and female germline lineages are established. Sufficient numbers (i.e. six) of unrelated F0 generation gestating females and males were used to generate an intercross and avoid any inbreeding [1, 29]. Inbreeding depression of epigenetics has been previously observed [30–32], so is avoided in epigenetic inheritance experimental models [1, 7]. The F3 generation males were aged to 5 months for sperm collection with optimal fertility and others to 1 year of age for pathology analysis. The sperm were stored at –80°C and shipped on dry ice in one shipment to Dr Wei Yan's *in vitro* fertilization laboratory for ICSI of wild-type control female SD rat oocytes, as described in the Methods. The ICSI-generated embryos from both the control and DDT lineage F3 generation sperm were incubated (i.e. 5 days) in culture until the morula embryo stage, and then, viability was assessed with microscopy (Fig. 1B and Supplementary Fig. S1). When adequate development and morphology were obtained, the morula embryos were collected and stored at –80°C. The morula embryos were pooled to generate three (pools) groups of 21–24 morula embryos each for analysis. The control and DDT lineage F3 generation sperm and morula embryos were the focus. ICSI morula embryos were also obtained from non-exposed lineage wild-type SD rats for ICSI procedure optimization and analysis. The frozen morula embryos were then shipped in a single shipment on dry ice to Dr Michael Skinner's Washington State University (WSU) laboratory and stored at –80°C until molecular analysis.

The sperm samples used to isolate individual sperm for ICSI were also used to generate three sperm pools from three males per group/pool to correlate with the three pools of ICSI embryos. The DNA was extracted from the sperm and morula embryo pools, as described in the Methods. A methylated DNA immunoprecipitation (MeDIP) was performed on each of the control and DDT sperm and ICSI morula embryo pools (three pools each total). Sequencing libraries were generated for each pool, and DNA sequencing was performed. A comparison between the sperm control versus sperm DDT was made to identify the sperm transgenerational DMRs, while the morula control and morula DDT comparison was made to identify the embryo DMRs (Fig. 2A and B). The DMRs at various edgeR statistical thresholds (*P*-values) are presented with transgenerational sperm control versus sperm DDT having 318 DMRs at $P < 1e\text{-}04$ (i.e. $P < 0.0001$) and transgenerational morula embryo control versus DDT DMRs having 425 DMRs at edgeR $P < 1e\text{-}04$ (Fig. 2A and B and Supplementary Tables S1 and S2). Further discussion of statistical significance with false discovery rates is presented in the Methods. A comparison of the DMRs with an increase (positive log) and a decrease (negative log) in methylation was ~50% for both sperm and morula (Fig. 2C and D). Approximately 50% of the sperm or morula control versus DDT DMRs had an increase in DNA methylation, and the remaining had a decrease in DNA methylation (Fig. 2E and F and Supplementary Tables S1 and S2). Only one DMR overlapped for both sperm and morula DMRs at $P < 1e\text{-}04$. However, the issue is not the similarity of the presence of a DMR but the maintenance of DNA methylation at the DMR sites. The sperm DMR methylated read depth was found to be retained in the morula. The methylated DMR site read depth was normalized for changes in DNA concentrations and for library size [i.e. reads per kilobase per million (RPKM)] to allow comparison of the samples. A graphic representation of the sperm DMR methylation in the morula is presented in Fig. 3A. Sperm DMR sites with an increase in DNA methylation generally had retention or a slight decrease in DNA methylation, while those sperm DMR sites with a decrease in methylation had an increase in methylation levels in the morula (Fig. 3A). The sperm DMR site DNA methylation was ordered based on read depth (black, Fig. 3B), and the corresponding morula DNA methylation read depth (red) was found to be retained or increased for 74% of the DMRs, retained with a small decrease (i.e. <50%) for 24% of the DMR sites, and not retained (i.e. <10%) for 2% of the sperm DMR sites (Fig. 3B and Supplementary Fig. S2). Therefore, of the 318 sperm DMR sites, 311 DMR sites (98%) retained methylated DNA read depth in the morula (Fig. 3A and B and Supplementary Fig. S2). Therefore, sperm DMR methylation read depth was primarily retained in the morula (Fig. 3A and B). Note that the sperm DMR site methylation read depth is retained in the morula embryo, even though by definition these are not significant DMRs in the morula. In conclusion, an analysis of 318 transgenerational sperm DMRs (i.e. control versus DDT DMRs) used read depth normalized to library size for RPKM and correlated this with the same sites in the morula embryo samples (Fig. 3A and B). Interestingly, the sperm control versus DDT DMR sites that had an increase transgenerationally maintained similar read depths in the morula. This was also shown with a comparison of sperm and morula read depth (Fig. 3B). Therefore, the DNA methylation at the 318 DMR sites was generally not erased but maintained or increased in the morula embryo.

Since imprinted genes have a DNA methylation imprint that escapes the DNA methylation erasure for the morula embryo, several paternal and maternal imprinted sites were evaluated to assess DNA methylation patterns in the current study data. An example of two paternal imprints (i.e. *Rasgrf1* and *Zdbf2*) is shown in Fig. 4A and B. Additional examples of both paternal and maternal imprints are also provided in Supplementary Fig. S3. Critical CpG methylation sites were examined and identified, and consistent DNA methylation (read depth) was observed in the

A Sperm Control vs Sperm DDT DMRs

p-value	All Window	Multiple Window
0.001	2128	48
1e-04	**318**	**14**
1e-05	68	6
1e-06	24	4
1e-07	10	4

Significant 1kb windows (p<1e-04)	1	2	3	4	5
Number of DMR	304	10	1	2	1

B Morula Control vs Morula DDT DMRs

p-value	All Window	Multiple Window
0.001	2816	15
1e-04	**425**	**1**
1e-05	76	1
1e-06	17	1
1e-07	2	0

Significant 1kb windows (p<1e-04)	1	2	3	4	5
Number of DMR	424	1	0	0	0

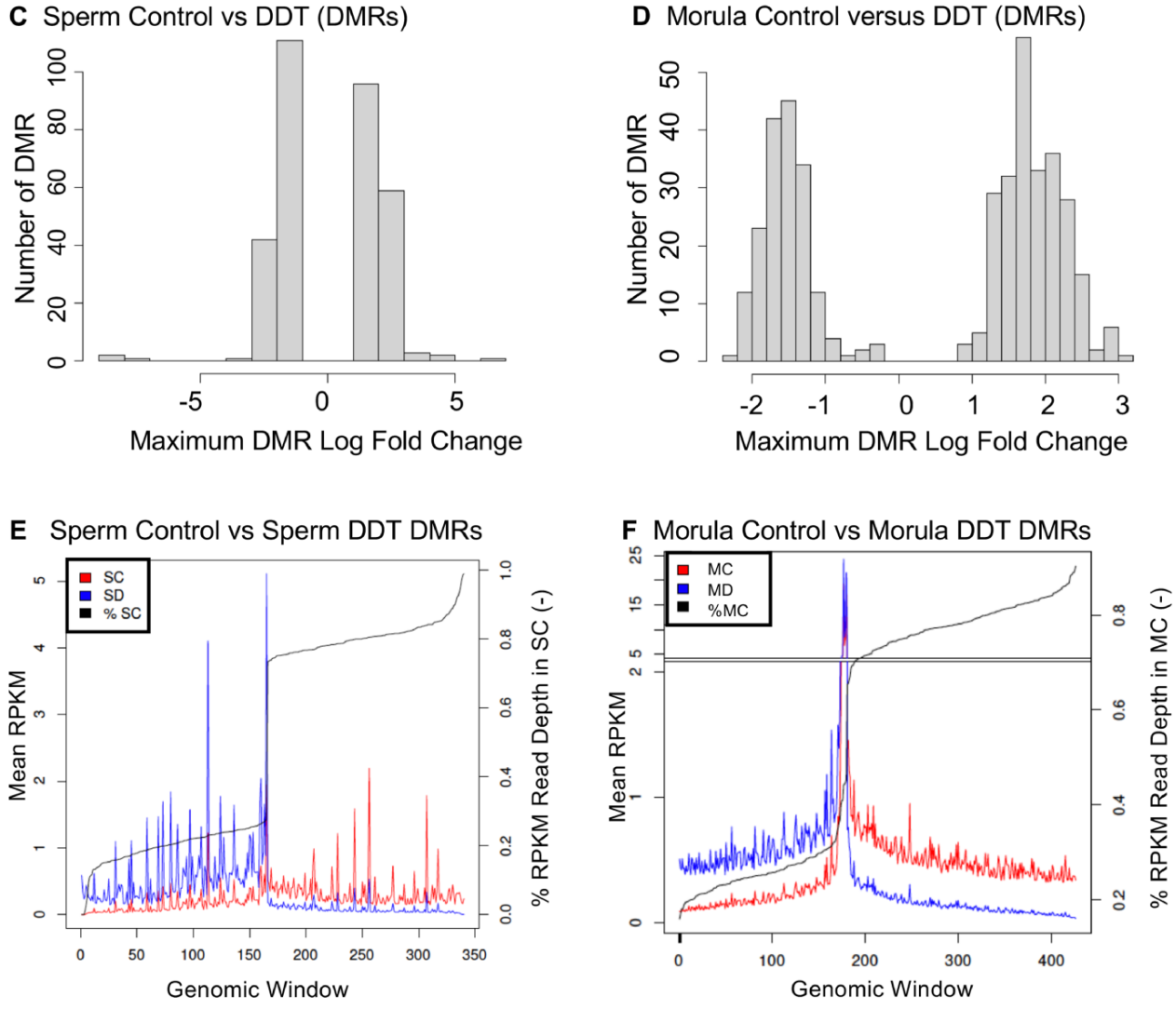

Figure 2: The differential DNA methylation analysis. **(A)** Sperm control versus sperm DDT DMRs at various edgeR *P*-values for 1 kb windows; **(B)** Morula embryo control versus morula DDT DMRs; DNA methylation alterations in DMRs; **(C)** Sperm control versus sperm DDT $P < 1e\text{-}04$ DMR numbers for maximum log fold change; **(D)** Morula control versus morula DDT DMR $P < 1e\text{-}04$; **(E)** Sperm control versus sperm DDT RPKM read depth; and **(F)** Morula control versus morula DDT mean RPKM. SC, sperm control; SD, sperm DDT; MC, morula control; MD, morula DDT. Three pools of sperm and morula embryos each from different animals were used for comparisons.

sperm and morula embryo for both the control and DDT exposure lineages (Fig. 4A and B and Supplementary Fig. S3). The gene location and conserved methylation sites were identified. Therefore, these validation observations support the protection and retention of DNA methylation in the imprinted sites with the molecular analysis and samples used in the current study.

A follow-up analysis used the MeDIP-Seq data to compare the sperm versus morula for both the control and DDT lineages (Fig. 5A and B). A large number of DMRs were identified at various edgeR *P*-values with 17 625 DMRs for control lineage and 19 733 DMRs for DDT lineage at $P < 1e\text{-}07$. The extended overlap at $P < 1e\text{-}07$ with $P < 0.05$ demonstrated 68–88% overlap between

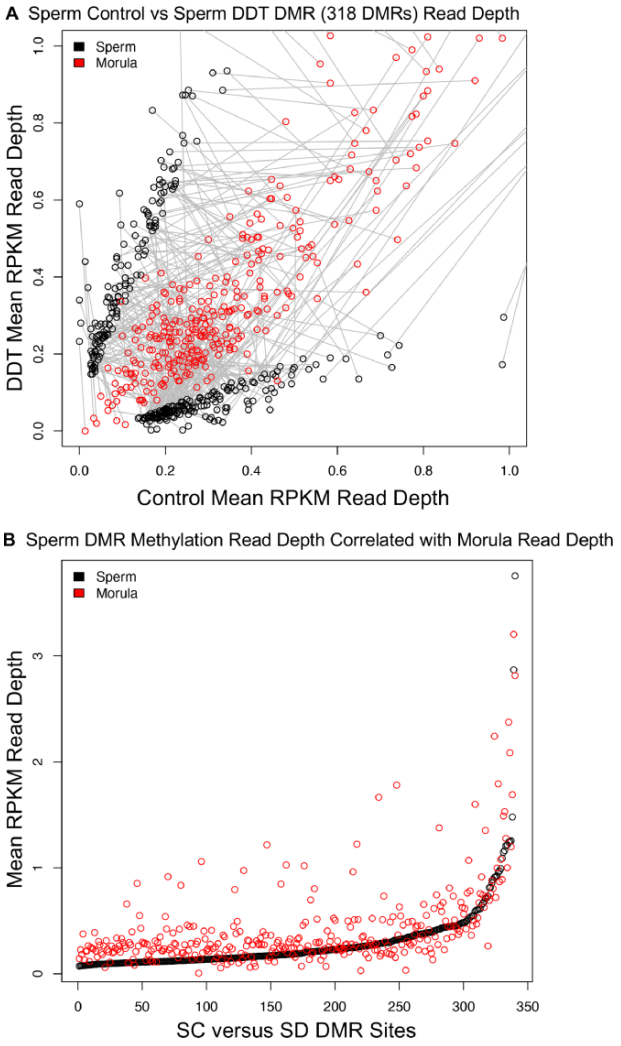

Figure 3: The sperm versus morula DNA methylation read depth comparison. **(A)** Sperm versus morula DMR (318 DMRs) methylation variation in sperm and morula for control and DDT DNA methylation mean RPKM read depth and **(B)** Mean RPKM read depth at sperm DMR DNA methylation sites in sperm (black) and morula (red). Sites have been ordered by mean read depth in sperm.

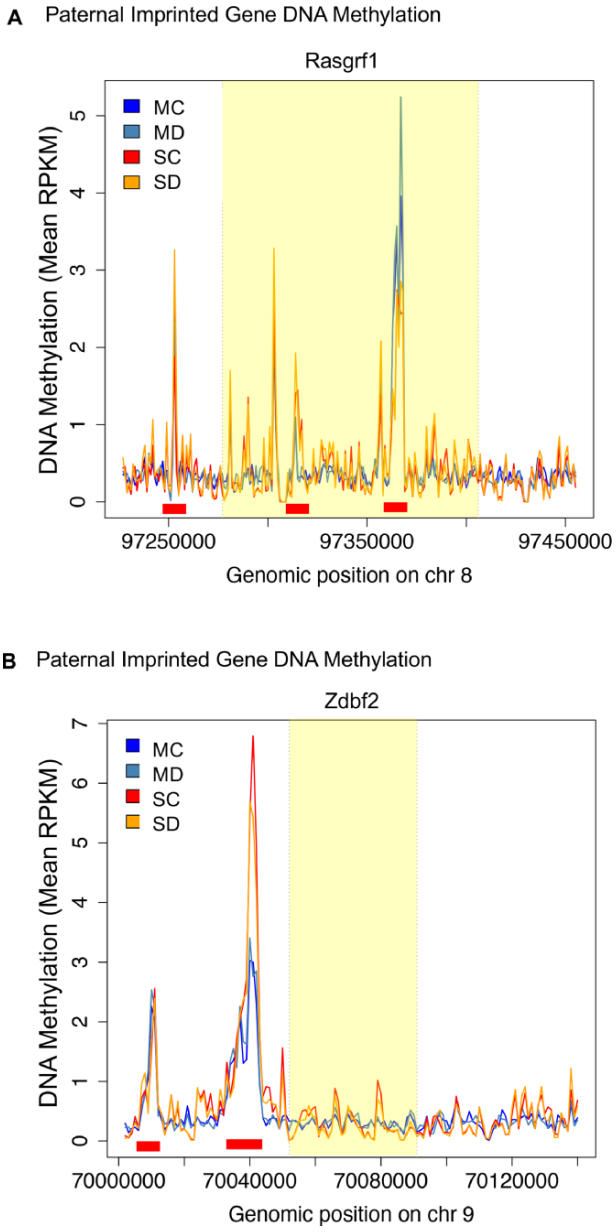

Figure 4: The sperm versus morula DNA methylation–imprinted gene site read depth comparison. **(A)** Paternal imprinted gene DNA methylation Rasgrf1 and **(B)** Paternal imprinted gene DNA methylation Zbdbf2. The gene body is shown with a yellow highlight. The red bar indicates the retention of methylation in sperm and morula.

the control and DDT lineage sperm versus morula DMRs (Fig. 5G). This demonstrates that the majority of DMRs between sperm and morula were common in both control and DDT lineages. Approximately 8–18% overlap was observed with the overlap of the sperm or morula comparisons alone, with the sperm versus morula comparisons. Interestingly, when the sperm versus morula DMRs were examined, the majority of the DMRs had an increase in DNA methylation in the morula embryo compared to the sperm for both control and DDT lineages (Fig. 5C and D). Greater than 90% of the DMRs had increased DNA methylation in the morula. Therefore, a significant increase in DNA methylation was observed between the sperm and morula for both control and DDT exposure lineages. An alternate raw read depth presentation of the changes in DNA methylation between the sperm and morula embryo is presented in Fig. 5E and F and Supplementary Fig. S4A–D. The sperm versus morula DMR sites for both the control and DDT lineages are presented and demonstrate that the vast majority of the DMRs in the morula have an increase in DNA methylation (Fig. 5A–F). The analysis with a raw read depth and normalized RPKM shows similar results (Supplementary Fig. S4). Therefore, a dramatic increase in DNA methylation between the sperm and morula embryo is observed for both the control and DDT lineages. The extended overlap with a low statistical threshold comparison at $P < 0.05$ demonstrates that between 68% and 88% of these DMRs are similar between the control and DDT lineages (Fig. 5G), suggesting a baseline increase in DNA methylation during morula embryo development that is similar.

The genomic features of the DMRs in the sperm and morula or comparison of sperm and morula (top 1000) is presented in Supplementary Tables S1–S4. The genomic locations are genome-wide (Supplementary Fig. S5) for all the analyses. There is good separation in a principal component analysis for all the comparisons (Supplementary Fig. S6). The CpG density of the DMRs for the sperm, morula, and sperm versus morula is all predominantly 1

A Sperm Control vs Morula Control DMRs

p-value	All Window	Multiple Window
0.001	202786	45436
1e-04	111195	18654
1e-05	59804	8427
1e-06	32080	4290
1e-07	**17625**	**2434**

B Sperm DDT vs Morula DDT DMRs

p-value	All Window	Multiple Window
0.001	192816	41076
1e-04	108433	17383
1e-05	59866	8218
1e-06	33414	4905
1e-07	**19733**	**3564**

C Sperm Control versus Morula Control DMRs

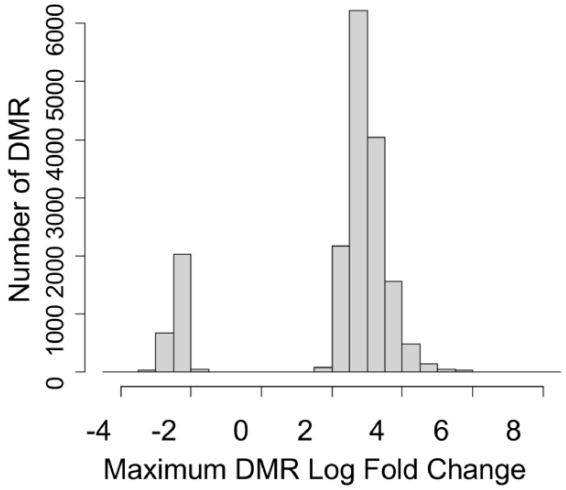

D Sperm DDT versus Morula DDT DMRs

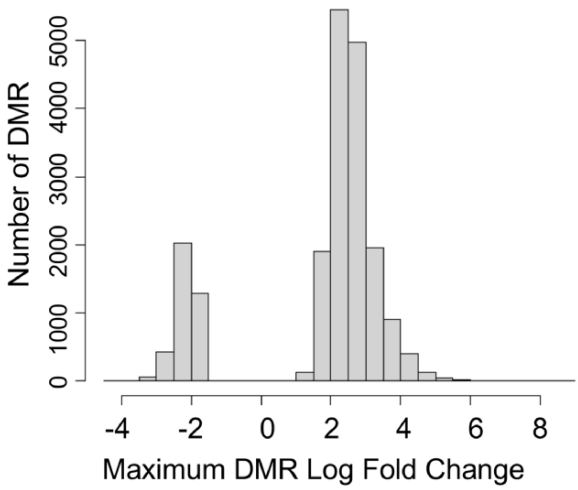

E Sperm Control vs Morula Control DMRs RPKM

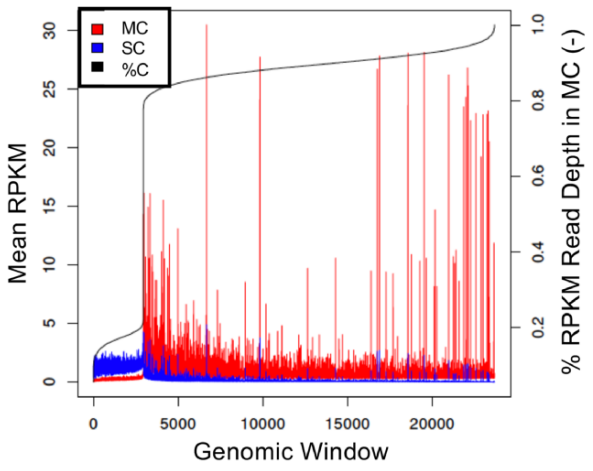

F Sperm DDT vs Morula DDT DMRs RPKM

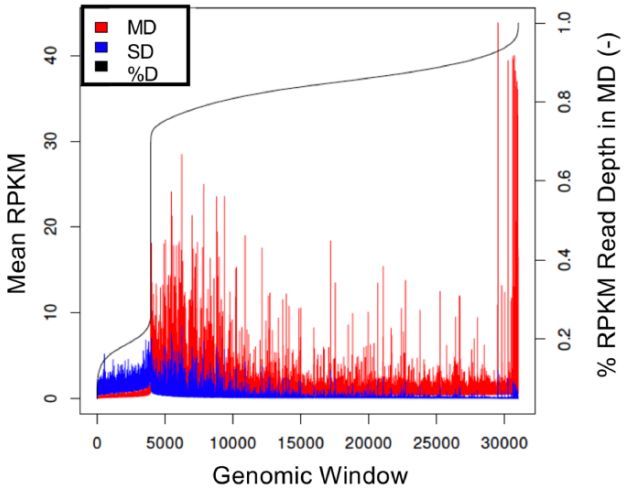

G Expanded DMR Overlap

p<0.05 / p<1e-04	SC vs SD	MC vs MD	SC vs MC	SD vs MD
SC vs SD	318 (100.0%)	23 (7.2%)	180 (56.6%)	103 (32.4%)
MC vs MD	12 (2.8%)	425 (100.0%)	189 (44.5%)	272 (64.0%)
SC vs MC	11799 (10.6%)	13705 (12.3%)	111195 (100.0%)	76296 (68.6%)
SD vs MD	8883 (8.2%)	20006 (18.5%)	95654 (88.2%)	108433 (100.0%)

Figure 5: The sperm versus morula DMR methylation comparison. **(A)** Sperm control versus morula control DMRs; **(B)** Sperm DDT versus morula DDT DMRs; **(C)** DMRs and log fold change sperm control versus morula control $P < 1e\text{-}07$; **(D)** DMRs and log fold change sperm DDT versus morula DDT $P < 1e\text{-}07$; **(E)** Sperm control versus morula control DMRs mean read depth $P < 1e\text{-}07$ (RPKM) per 1 kb genomic windows; **(F)** Sperm DDT versus morula DDT DMRs (RPKM); **(G)** Expanded DMR overlap at $P < 1e\text{-}04$ DMRs versus comparison presence at $P < 0.05$. The overlapping $P < 1e\text{-}04$ versus $P < 0.05$ DMRs number and percent overlap are indicated. SC, sperm control; SD, sperm DDT; MC, morula control; MD, morula DDT.

CpG/100 bp (Fig. 6A–D). The DMRs are predominantly 1 kb in size (Supplementary Fig. S7A–D). Therefore, the DMR sites observed in the current study with the MeDIP-Seq protocol are in low-density CpG regions (i.e. CpG deserts) [33]. Previously, MeDIP-Seq has been shown to be biased to low-density CpG in the 1–5 CpG/100 bp, while the bisulfite sequencing has a bias for higher-density CpG of >5 CpG/100 bp CpG islands (CGIs) [34–36]. These data are also shown in Fig. 6 [34], where the rat genome is shown to have a CpG density of predominantly 1 CpG/100 bp, followed by 2 and 3 CpG/100 bp that constitutes ∼90% of the genome sequence (Fig. 6E). Similar observations are observed with the human genome (Supplementary Fig. S7E and F). The MeDIP analysis is biased toward the detection of DNA methylation at densities of 1–4 CpG/100 bp, while bisulfite sequencing (i.e. whole-genome bisulfite or reduced representation bisulfite) is biased to detect methylation at higher densities of >5 CpG/100 bp (Fig. 6G and H) [34]. This is similar for human DNA methylation analyses as well (Supplementary Fig. S6E and F). This bias in MeDIP is due to antibody-binding specificity being interfered with at higher-density CpG [37]. Bisulfite-based methods are biased in part due to the bioinformatics protocols used that screen out low-density CpG regions of the genome from the analysis [38, 39]. To put this in perspective to the sperm and morula DMRs observed in the current study, the genome-wide RPKM DMR read depth versus CpG for 1 kb average (CpG/100 bp) is presented in Fig. 7A. The morula had higher levels of DMR methylation at 0.1–1.0 CpG/100 bp and >4.5 CpG/100 bp, in which the sperm were higher than morula at >1 CpG/100 bp to <4 CpG/100 bp. Therefore, the sperm and morula methylation patterns are unique.

The DMR-associated gene functional categories for each of the comparisons are presented in Fig. 8A. The frequency of DMRs for each gene functional category is identified. Similar observations are presented for each comparison except the sperm DDT versus morula DDT DMR-associated gene categories. The final analysis involved DMR associations with genes. Supplementary Tables S1–S4 present the specific DMR-associated genes and functional gene categories. Approximately 50% of the DMRs have gene associations within 10 kb, such that distal and proximal gene promoter regions are considered. The locations of the DMR with respect to genes demonstrated for all DMR comparisons ∼40% in intergenic regions, 15% in promoter and enhancer regions, 46% in gene bodies, and 30% repeat elements when ≥50% of the DMR sequence had repeat elements. KEGG pathway analyses show those pathways with the largest number of genes (in brackets) for sperm control versus sperm DDT, morula control versus morula DDT, sperm control versus morula control (top 1000 DMR), and sperm DDT versus morula DDT (Fig. 8B–E). Outside major common pathways such as metabolism and cancer, there were none observed for the different associated gene sets. Therefore, the DMRs identified did have extensive gene associations and potentially affect multiple gene pathways. No significant repeat element composition of the DMR sites versus the whole-genome composition was observed (Fig. 7). Therefore, the 1 kb DMRs had ∼30% repeat element composition when ≥50% of the DMR sequence had repeat element sequence present. Therefore, the DMRs and methylation retention sites appear primarily independent of any significant repeat element composition.

Discussion

The current literature has promoted the concept that the erasure of DNA methylation occurs during early embryonic development to generate the pluripotent embryonic stem cells [12, 40]. This has developed from observations that CGIs with high-density CpG density (i.e. >5–10 CpG/100 bp) DNA methylation are erased [41]. The general technology used to establish these observations in the vast majority of previous studies involved bisulfite sequencing [12, 41]. During embryonic development following fertilization, the early embryo progressing with each cell division erases the majority of CGI methylation to the lowest level in the morula embryo stage [41] (Fig. 1A). The other developmental period where CGI erasure is observed is the primordial germ cells during genital ridge migration and prior to gonadal sex determination for the primordial germ cell to become pluripotent [12]. The proposed function of this DNA methylation erasure in the embryo is to generate the pluripotent stem cells in the morula embryo to subsequently generate all developing somatic cell types with cell-specific DNA methylation [12, 41].

An exception previously established for the DNA methylation erasure involves imprinted genes that are protected from this DNA methylation erasure during stem cell development [14, 42, 43]. Recently, the presence of tripartite motif–containing protein 28 [16] and the Kruppel-associated box domain family zinc finger proteins (e.g. Krb28) at the imprinted gene sites appears to have a role in protecting the sites from DNA methylation erasure [17, 18]. Therefore, mechanisms exist to facilitate the escape from DNA methylation erasure during early embryo development [17, 44]. The current study supports the maintenance of DNA methylation on a variety of imprinted sites in a comparison of sperm versus morula methylation levels using MeDIP followed by next-generation sequencing (MeDIP-Seq). This validated that imprinted genes are protected from DNA methylation erasure during early embryonic development (Fig. 4 and Supplementary Fig. S3).

Epigenetic transgenerational inheritance is a non-genetic environmental responsive process for the germline (egg and sperm) to transmit molecular alterations to subsequent generations (e.g. great-grand offspring, F3 generation) [1, 7]. Although all forms of epigenetics (e.g. DNA methylation, histone modifications, and non-coding RNA) are involved [8], the current study focused only on alterations in DNA methylation. In the initial observation of epigenetic transgenerational inheritance [1], the speculation was made that sperm DMRs would be protected from DNA methylation erasure as imprinted-like genes [1, 20]. The current study obtained sperm from F3 generation control and DDT exposure lineage male rats and used the sperm in ICSI to generate morula embryos in culture that contain the totipotent stem cells. Observations indicate that the F3 generation DDT-induced DMRs in sperm escaped DNA methylation erasure and often increased in DNA methylation in morula (Figs 1–3 and Supplementary Fig. S4). The sperm DMRs that had decreased methylation due to ancestral DDT exposure often had increased DNA methylation in the morula embryo (Fig. 5). Although an optimal comparison with the morula would have been the zygote instead of the sperm, it was not possible to collect sufficient amounts of zygotes for the molecular analysis. Therefore, sperm were used due to the high levels of cells available. In examining the DDT-induced transgenerational sperm DMRs, the DNA methylation was retained or increased in the morula stem cell populations. Therefore, the current study confirms that the environmentally induced transgenerational DMRs in sperm maintained or increased their altered DNA methylation in the embryonic stem cells. As previously speculated [20], they act as imprinted-like genes to transmit an altered epigenome and transcriptome to the morula stem cells to subsequently impact the epigenetics and transcriptome of all subsequently derived somatic cell populations.

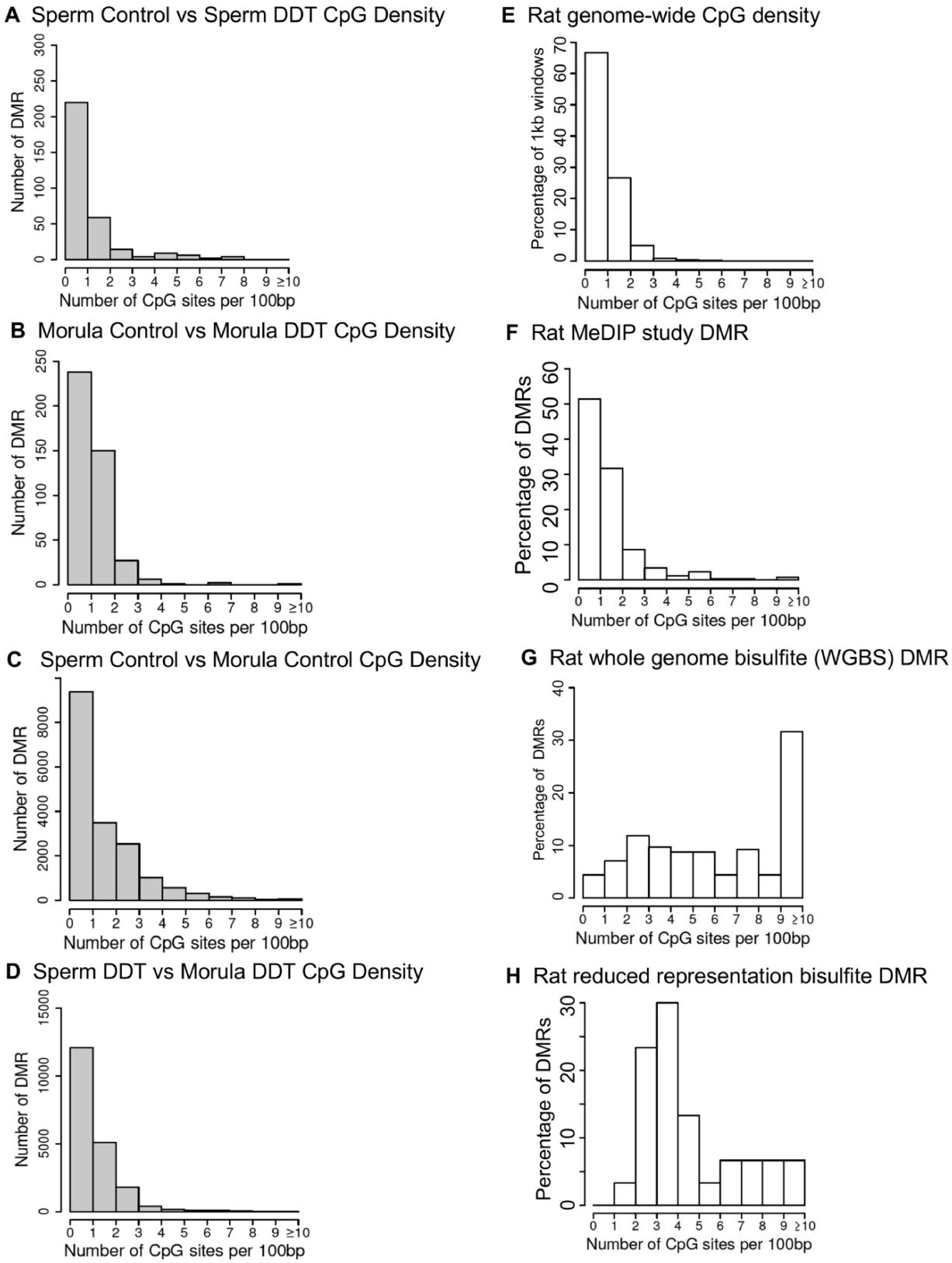

Figure 6: DMR CpG density and method limitations. **(A)** Sperm control versus sperm DDT CpG density (number of sites per 100 bp); **(B)** Morula control versus morula DDT CpG density; **(C)** Sperm control versus morula control CpG density; **(D)** Sperm DDT versus morula DDT CpG density. Genome-wide CpG density; (**E**) Rat whole-genome CpG density per 100 bp; **(F)** Analysis percentage DMRs and CpG density rat genome with MeDIP sequencing (MeDIP-Seq); **(G)** Rat whole-genome bisulfite (WGBS). The percentage of DMRs corresponded to the number of CpG sites per 100 bp rat WGBS study DMR; and **(H)** Reduced representation bisulfite (RRBS) percentage of DMRs corresponded to the number of CpG sites per 100 bp rat RRBS study DMR. These data were obtained from the reference [34] of the authors with a modified presentation to put in perspective of the current study data.

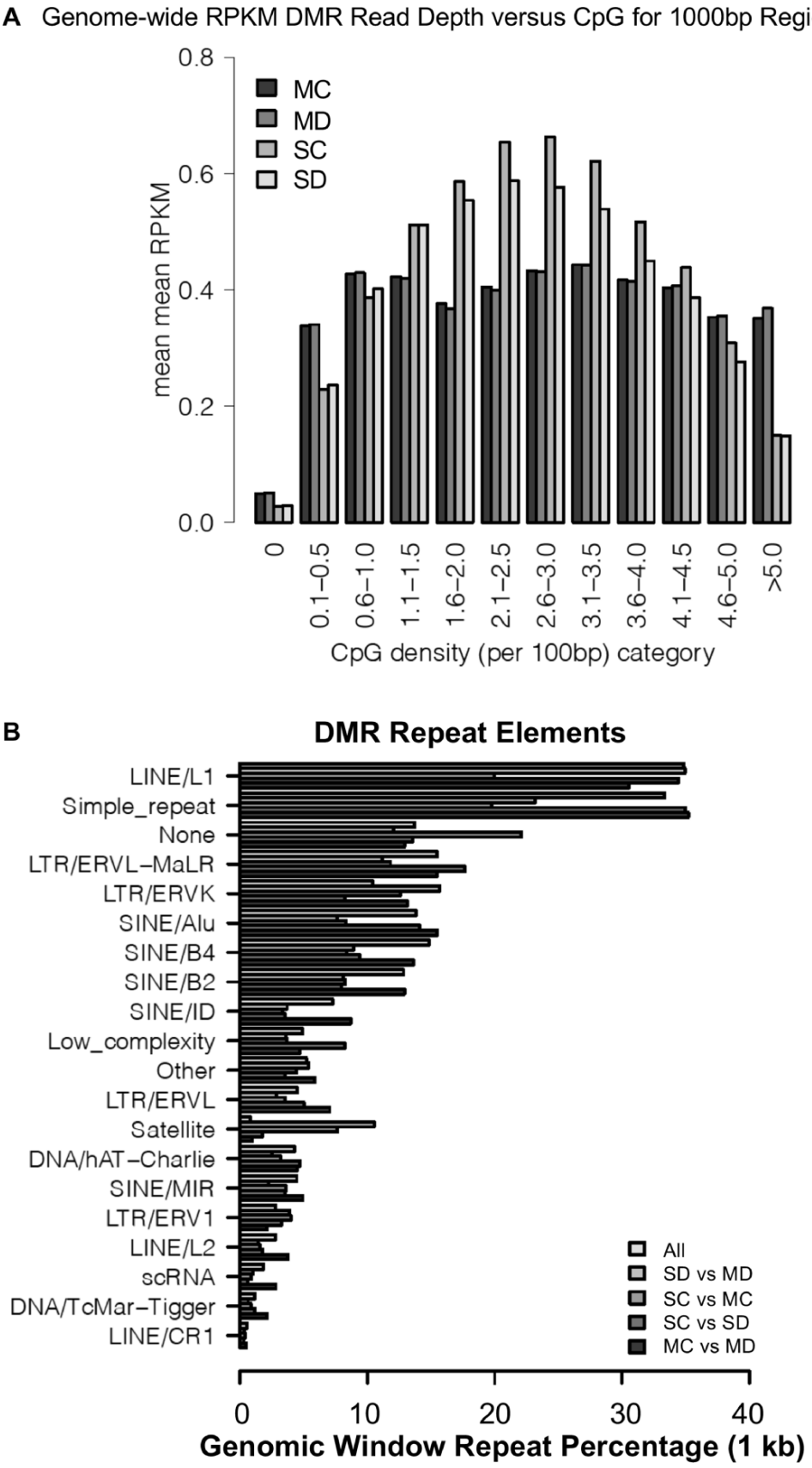

Figure 7: Genome-wide DMR and repeat elements. **(A)** Genome-wide DMR read depth RPKM versus CpG density for 1 kb regions average (CpG/100 bp). Morula control (C), DDT (D), sperm control (SC), and sperm DDT (SD). **(B)** DMR gene associations and repeat elements. DMR repeat element frequency (%) present compared to whole-genome-wide frequency with 1 kb window genomic sites. SC, sperm control; SD, sperm DDT; MC, morula control; MD, morula DDT, and all genome-wide. The DMR for SC versus SD and MC versus SD at $P < 1e\text{-}04$, SC versus MC and SD versus MD at $P < 1e\text{-}07$, and genome-wide 1 kb windows.

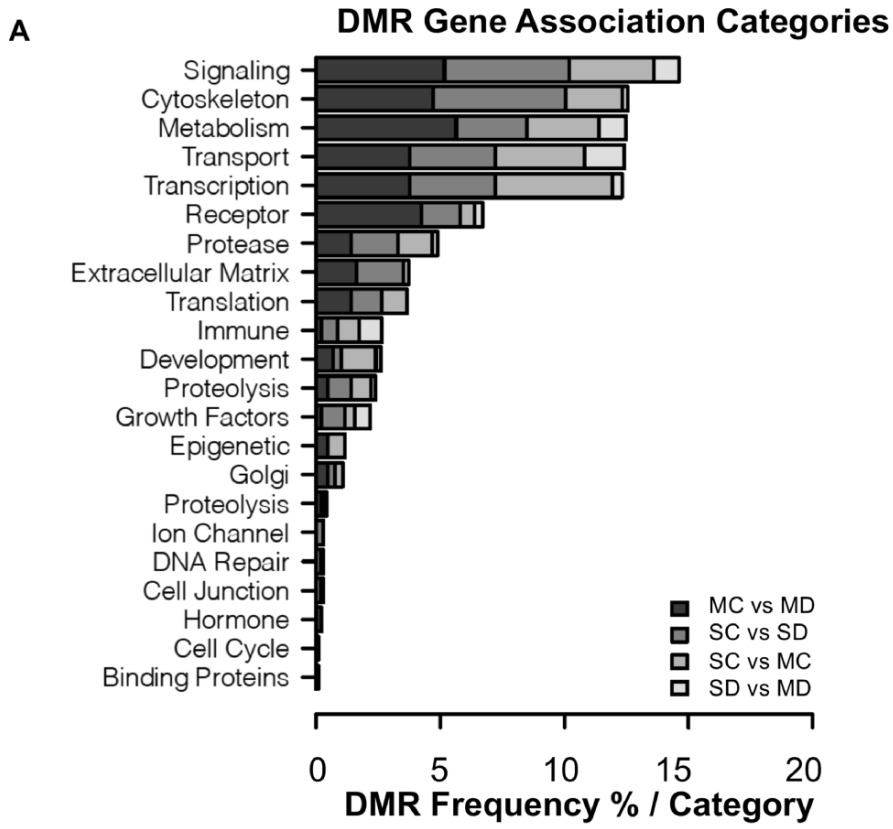

B SC versus SD p<1e-04 DMR

rno01100 Metabolic pathways (10)
rno04740 Olfactory transduction (8)
rno05200 Pathways in cancer (7)
rno04020 Calcium signaling pathway (6)
rno04144 Endocytosis (5)
rno05010 Alzheimer disease (5)
rno05022 Pathways of neurodegeneration (5)
rno04310 Wnt signaling pathway (5)
rno05020 Prion disease (4)
rno05016 Huntington disease (4)

C MC versus MD p<1e-04 DMR

rno01100 Metabolic pathways (19)
rno05200 Pathways in cancer (14)
rno04151 PI3K-Akt signaling pathway (10)
rno05165 Human papillomavirus infection (9)
rno04740 Olfactory transduction (9)
rno04360 Axon guidance (8)
rno04010 MAPK signaling pathway (7)
rno04024 cAMP signaling pathway (7)
rno04022 cGMP-PKG signaling pathway (7)
rno05171 Coronavirus disease - COVID-19 (7)

D SC versus MC top 1000 DMR

rno01100 Metabolic pathways (27)
rno05200 Pathways in cancer (17)
rno05167 herpesvirus infection (13)
rno05163 Human cytomegalovirus infection (13)
rno04010 MAPK signaling pathway (12)
rno04144 Endocytosis (12)
rno04390 Hippo signaling pathway (11)
rno05166 T-cell leukemia virus 1 infection (11)
rno05168 Herpes simplex virus 1 infection (10)
rno05022 Pathways of neurodegeneration (10)

E SD versus MD top 1000 DMR

rno04144 Endocytosis (9)
rno04612 Antigen processing and presentation (8)
rno05166 T-cell leukemia virus 1 infection (7)
rno05168 Herpes simplex virus 1 infection (7)
rno04145 Phagosome (7)
rno05163 Human cytomegalovirus infection (6)
rno04218 Cellular senescence (6)
rno01100 Metabolic pathways (6)
rno05165 Human papillomavirus infection (5)
rno04940 Type I diabetes mellitus (5)

Figure 8: DMR gene associations. **(A)** DMR gene association functional categories. SC, sperm control; SD, sperm DDT; MC, morula control; MD, morula DDT, and all genome-wide. The DMR for SC versus SD and MC versus SD at $P < 1e\text{-}04$, SC versus MC and SD versus MD at $P < 1e\text{-}07$, and genome-wide 1 kb windows. DMR-associated gene pathway analysis. **(B)** SC (sperm control) versus SD (sperm DDT) $P < 1e\text{-}04$; **(C)** MC (morula control) versus MD (morula DDT) $P < 1e\text{-}04$; **(D)** SC versus MC top 1000 DMRs; and **(E)** SD versus MD top 1000 DMRs. The pathway listed and DMR-associated gene numbers in brackets.

The environmentally induced epigenetic transgenerational inheritance of the imprinted-like DMRs in the early embryo allows the transgenerational transmission of epigenetic information generationally [12, 20]. All organisms examined have epigenetic transgenerational inheritance of phenotypic alterations due to the reprogramming of the basal epigenetics of the stem cell populations [45, 46]. Previous literature supports this concept and suggests that various epigenetic factors such as ncRNA, histone modification, and DNA methylation are involved [8]. Although the epigenetic alterations in the germline being passed to the early embryo have not been generally investigated, the concept that such events occur has been proposed [1, 12, 45, 46].

A recent study compared a number of different molecular procedures to analyze DNA methylation in a genome-wide manner [34]. Previous studies have also compared molecular procedures to look for biases in the analyses [34–36]. Bisulfite procedures have been extensively used followed by next-generation sequencing (BS-Seq) to assess genome-wide DNA methylation in early embryonic development [34, 47]. This has led to the concept that DNA methylation erasure occurs during early embryo development and primordial germ cell development [12] (Fig. 1A). A limitation with BS-Seq is that it is often biased toward detecting changes in higher-density CpG sites such as CGIs with >5 CpG/100 bp [34–37]. An analysis of the mammalian genome in rats and humans demonstrates that <5% of the genome contains CGIs [34] (Fig. 6 and Supplementary Fig. S7). Therefore, the previous analyses regarding DNA methylation erasure are primarily limited to high-density CpG (i.e. CGI) [48], as more recently reviewed [34]. A critical technical limitation to BS-Seq is that the bioinformatics protocols used remove low-density (<3 CpG/100 bp) regions from the genome prior to analysis [38, 39]. In contrast, MeDIP-Seq analysis is biased to low-density CpG sites with <5 CpG/100 bp that constitute >90% of the genome [34] (Fig. 6 and Supplementary Fig. S6). Therefore, the previous studies with BS-Seq very accurately assess CGIs and support the extensive literature on the erasure of DNA methylation during early development [12, 48]. However, the analysis of the >90% of the genome to assess lower-density CpG deserts [34] has not been rigorously assessed and may benefit from procedures such as MeDIP-Seq.

The current study using MeDIP-Seq and the analysis of >90% of the genome surprisingly demonstrated that the majority of sperm DMR methylation at the low-density sites has an increase in DNA methylation in the morula embryo (Fig. 5 and Supplementary Fig. S4). This was observed in both the control lineage sperm and morula comparison and the DDT lineage comparison (Fig. 5A–F). An extended overlap of the two lineages demonstrated 68–88% overlap of the sperm versus morula DMRs but <10% overlap with the control versus DDT sperm or morula DMRs (Fig. 5G). Observations suggest that the majority of the genome with low-density CpG deserts has an increase in DNA methylation in the morula embryo. This is in contrast to the current concept based on CGI analysis of DNA methylation erasure [12, 48, 49] (Fig. 1A). The previous literature primarily utilizes bisulfite sequencing compared with the current study that uses MeDIP-Seq. The previous literature and observations were focused on CGIs and did not assess the majority (>90%) of the genome having low-density CpG <5 CpG/100 bp. A re-evaluation of this dogma of DNA methylation erasure is needed that considers the CpG density and technical procedures utilized.

A potential limitation to data interpretation to consider is whether the data obtained were biased to specific genomic features. A significant component of the genome involves repeat elements with often low-density CpG regions. Therefore, observations could be impacted if the low-density CpG sites observed with an increase in DNA methylation were biased to repeat elements. To assess this, the repeat elements present in the sperm versus morula DMRs were assessed and compared to those in a whole genome (Fig. 7). The distribution of the DMR-associated repeat elements was similar to that of the whole genome in regards to the percent repeat elements. In addition, the percent of the 1 kb DMRs containing repeat element has <30% when the DMR contained ≥50% repeat element sequence. Therefore, a bias to repeat elements was neither observed nor impacted the observations presented. Limitations of the current analysis do involve a limited number of samples of morula and sperm comparisons. Although several years of ICSI and morula development collection experiments were required to obtain the materials for the current study, more studies are now needed to replicate the observations in other species and with other environmental exposures. An additional limitation is that zygotes were not used for comparison; however, the inability to obtain sufficient zygotes with the methods used prevented this comparison, and the sperm transmission of the transgenerational DMRs was the focus of the current study. The potential use of ICSI compared to normal *in vitro* fertilization would be interesting in the future to assess the potential impacts of ICSI. The technologies for the study have all been well established [34], and the bioinformatic analyses used, and normalization procedures minimize any PCR artifacts or low DNA levels when observed. Therefore, the bioinformatics of read depth differences are corrected. Future studies are needed to confirm that technical artifacts are not generated in the normalization procedures. In addition, different cell types were compared, and this needs to be considered in data analysis and interpretation. Further analyses of other developmental stages of embryonic development from the two to four cell embryos to the blastula will also help better understand the phenomenon observed. As a validation experiment, wild-type control embryos were generated and compared with the control lineage sperm for analysis. Similar observations of an increase in low-density CpG DMRs were observed. Although further studies are needed, the current study provides unique observations that suggest that a re-evaluation of the dogma of DNA methylation erasure of the whole genome is now needed.

In conclusion, the current study demonstrates that many transgenerational sperm DMRs maintain or increase their DNA methylation levels between the sperm and morula stages of embryonic development. This supports the previous proposal that early embryo epigenetics and transcriptomes are impacted by environmentally induced epigenetic transgenerational phenomenon [1, 45]. Therefore, the transgenerational DMRs appear imprinted-like and maintain DNA methylation to transmit the subsequent generation transgenerational phenotypes [1, 20, 45]. Interestingly, using MeDIP-Seq with a focus on lower-density CpG demonstrated that a large percentage of the morula genome had an increase in DNA methylation. The various experiments and controls support this observation, but further studies are needed. Observations suggest that embryo development has a more dynamic regulation of the epigenome with low-density CpG increase in methylation and high-density CGI decreases in DNA methylation. The function of the low-density CpG deserts' increase in DNA methylation remains to be determined but appears to complement the DNA methylation erasure of CGIs. The observations indicate that the transgenerational inheritance of DMR methylation is maintained such that they can alter the DNA methylation and transcriptomes of the early embryonic stem cells. This will include both decreases in higher-density

CpG sites and increases in low-density CpG sites. The alteration of the morula stem cell epigenetics will subsequently impact the epigenomes and transcriptomes of all subsequently derived somatic cells in the organism. This provides the molecular basis for the epigenetic transgenerational inheritance phenotypes and pathologies observed [45]. Future studies need to re-evaluate the current dogma of a genome-wide erasure of DNA methylation and consider a more dynamic regulation of early stem cell epigenetic development in the embryo.

Methods

Animal studies and breeding

As previously described [21–27], female and male rats of an outbred strain Hsd:Sprague Dawley SD (Harlan) at 70–100 days of age were fed *ad lib* with a standard rat diet and *ad lib* tap water. All animal cages were housed in the same room and environment with gestating females, and females with litters being housed individually within cages. Conditions were designed to minimize differences that would cause maternal effects. The breeding of unrelated males and females within specific exposure lineages (interbreeding) was used to optimize the maternal and paternal lineage contributions to the phenotypes observed [50]. No inbreeding within the colonies was performed. Previous studies have demonstrated inbreeding suppression of epigenetics [30–32]. Generally, six unrelated breeding pairs at the F0 generation were used to generate the subsequent generations. Timed-pregnant females were mated, and on embryonic Days 8 through 14 (E8–E14) of gestation, daily intraperitoneal injections of the treatment compound (DDT) (25 mg/kg) or vehicle control dimethyl sulfoxide were administered as previously described [29].

The gestating female rats exposed were designated as the F0 generation. F1–F3 generation control and exposure lineages were housed in the same room and racks with lighting, food, and water. Non-littermate females and males aged 70–100 days from the F1 generation of exposure or control lineages were bred within their treatment group to obtain F2 generation offspring. Unrelated F2 generation rats were bred to obtain F3 generation offspring. No sibling or cousin breeding was used to avoid any inbreeding artifacts. Only the F0 generation received exposure treatments. All animals were aged to 5 months for sperm collection for ICSI and epigenetic analysis and 1 year for pathology analysis. Animals were euthanized by use of a CO_2 chamber, followed by cervical dislocation as a secondary method. All experimental protocols for the procedures with rats were pre-approved by the Washington State University Animal Care and Use Committee (IACUC approval #2568 and 6931). All methods were performed in accordance with the relevant IACUC and Animal Research: Reporting of In Vivo Experiments (ARRIVE) guidelines and regulations.

Epididymal sperm collection

The protocol used is as previously described [8]. Briefly, the epididymis was dissected free of fat and connective tissue and then, after cutting open the cauda, placed into 6 ml of phosphate-buffered saline for 20 min at room temperature. Further incubation at 4°C will immobilize the sperm. The tissue was then minced, the released sperm pelleted at 4°C 3000 × *g* for 10 min, then resuspended in 250 µl NIM buffer, and stored at –80°C for ICSI or further processing.

ICSI and embryo collection

Adult female SD rats at 6–12 weeks of age with body weight >125 g were used as egg donors. These females were superovulated by intraperitoneal injection of 300 IU/kg of pregnant mare's serum gonadotropin, followed by intraperitoneal injection of 300 IU/kg of human chorionic gonadotropin 48 h later. Mature oocytes (MII stage) were collected from the oviducts 16 h after chorionic gonadotropin injection and freed from cumulus cells by treatment with 0.1% bovine testicular hyaluronidase (Sigma, Cat# H3506) in the M2 medium (Millipore, Cat# MR-015-D) at 37°C for 5 min. The cumulus-free oocytes were washed and kept in the KSOM–AA medium (Millipore, MR-121-D) in an incubator (Sanyo, Cat# 19AIC) at 37°C with air containing 5% CO_2 before ICSI.

ICSI was performed as described previously [51], with minor modifications. In brief, sperm frozen in TE buffer (10 mM Tris and 1 mM EDTA, pH 8.0) were thawed at 37°C for 3 min. An aliquot of 2 µl sperm TE suspension was mixed immediately with 50 µl of 4% PVP (Sigma, Cat# P5288) in water (Millipore, Cat# TMS-006-C). A single sperm head was picked up and injected into the mature oocytes using a glass pipette equipped with a piezo drill under the control of an electric micromanipulator (TransferMan NK2, Eppendorf). Injected oocytes were then transferred to the KSOM+AA medium (Millipore, Cat# MR-121-D) covered by mineral oil and cultured in an incubator at 37°C with humidified air containing 5% CO_2. After 24 h of culture in KSOM+AA, embryos were transferred into mR1ECM (Cosmo, CSR-R-M191) for further incubation. Morula stage embryos were collected at 100–104 h post ICSI into cryovials (Olympus, Cat#: 27-125), which were snap-frozen in liquid nitrogen followed by storage at –80°C until shipment on dry ice for MeDIP-Seq. Embryo development was observed at 100–104 h and 116–120 h after ICSI, and morula stage embryos were collected into cryovials (Olympus, Cat#: 27-125), which were snap-frozen in liquid nitrogen followed by storage at –80°C until shipment on dry ice for MeDIP-Seq. A single overnight shipment of all morula embryo vials on dry ice was used to transfer the ICSI embryos to the Skinner Laboratory at Washington State University. A total of 47 vials and 67 morula embryos were shipped for DDT lineage F3 generation embryos and 73 morula embryos for control lineage F3 generation embryos. Three pools of 21–24 embryos were made for each control and exposure lineage for molecular analysis. All methods were approved by the University of Nevada Reno Animal Care and Use Committee (IACUC #00494) and performed in accordance with the relevant IACUC and ARRIVE guidelines.

DNA isolation

For molecular analysis, an appropriate amount of rat sperm suspension (~50 µl) was used for DNA extraction. Previous studies have shown that mammalian sperm heads are resistant to sonication unlike somatic cells [52, 53]. Somatic cell contamination and debris were removed by brief sonication (Fisher Sonic Dismembrator, model 300, power level 25), which destroys the somatic cells and then centrifuged and washed one to two times in 1X phosphate-buffered saline. The resulting purified sperm pellet was resuspended in 820 µl DNA extraction buffer, and 80 µl 0.1 M DTT was added and then incubated at 65°C for 15 min. Proteinase K (80 µl of 20 mg/ml) was added, and the sample was incubated at 55°C for 2–3 h under constant rotation. Protein was removed by the addition of protein precipitation solution (300 µl, Promega A795A), incubated for 15 min on ice, and then centrifuged at 13 500 × *g* for 30 min at 4°C. One milliliter of the supernatant was precipitated with 2 µl of GlycoBlue (Invitrogen, AM9516) and 1 ml of cold 100% isopropanol. After incubation, the sample was spun at 13 500 × *g* for 30 min at 4°C and then washed with 70% cold ethanol. The pellet was air-dried for ~5 min and then resuspended in 100 µl of nuclease-free water.

MeDIP

The frozen –80°C sperm and morula embryo samples were prepared as previously described [8]. Genomic DNA was sonicated and run on 1.5% agarose gel for fragment size verification. The sonicated DNA was then diluted with 1X TE buffer to 400 µl, then heat-denatured for 10 min at 95°C, and immediately cooled on ice for 10 min to create single-stranded DNA fragments. Then, 100 µl of 5X IP buffer and 5 µg of antibody (monoclonal mouse anti-5-methyl cytidine; Diagenode #C15200006) were added, and the mixture was incubated overnight on a rotator at 4°C. The following day, magnetic beads (Dynabeads M280 Sheep anti-Mouse IgG; Life Technologies 11201D) were pre-washed per manufacturer's instructions, and 50 µl of beads were added to the 500 µl of DNA–antibody mixture from the overnight incubation and then incubated for 2 h on a rotator at 4°C. After the incubation, the samples were washed three times with 1X IP buffer using a magnetic rack. The washed samples were then resuspended in 250 µl digestion buffer (5 mM Tris at pH 8, 10 mM EDTA, and 0.5% SDS) with 3.5 µl proteinase K (20 mg/ml) and incubated for 2–3 h on a rotator at 55°C. DNA clean-up was performed using phenol–chloroform–isoamyl-alcohol extraction, and the supernatant was precipitated with 2 µl of GlycoBlue (20 mg/ml), 20 µl of 5 M NaCl, and 500 µl ethanol in –20°C freezer for one to several hours. The DNA precipitate was pelleted, washed with 70% ethanol, then dried, and resuspended in 20 µl H_2O or 1X TE. DNA concentration was measured in a Qubit apparatus (Life Technologies) with the ssDNA analysis kit (Molecular Probes Q10212).

MeDIP-Seq analysis

MeDIP DNA was used to create libraries for next-generation sequencing using the NEBNext Ultra RNA Library Prep Kit for Illumina (San Diego, CA) starting at Step 1.4 of the manufacturer's protocol to generate double-stranded DNA from the single-stranded DNA resulting from MeDIP. After this step, the manufacturer's protocol was followed indexing each sample individually with NEBNext Multiplex Oligos for Illumina. The WSU Spokane Genomics Core sequenced the samples on the Illumina HiSeq 2500 at PE50, with a read size of ~50 bp and ~100–150 million reads per pool. Two or three libraries were run in one lane.

Statistics and bioinformatics

The DMR identification and annotation methods follow those presented in previously published papers [8, 27]. Data quality was assessed using the FastQC program (https://www.bioinformatics.babraham.ac.uk/projects/fastqc/). The data were cleaned and filtered to remove adapters and low-quality bases using Trimmomatic [54]. The reads for each MeDIP sample were mapped to the Rnor 6.0 rat genome using Bowtie2 [55] with default parameter options. The mapped read files were then converted into sorted BAM files using SAMtools [56]. The MEDIPS R package [57] was used to calculate differential coverage between sample groups. The edgeR *P*-value [58] was used to determine the relative difference between the two groups for each genomic window. Windows with an edgeR *P*-value less than the selected $P < 1e\text{-}04$ threshold or $P < 1e\text{-}07$ for sperm versus morula were considered DMR. The site edges were extended until no genomic window with an edgeR *P*-value <0.1 remained within 1000 bp of the DMR. The edgeR *P*-value was used to assess the significance of the DMR identified. A false discovery rate analysis for each comparison was performed and provided $P < 0.1$ for the sperm versus morula comparisons and $P < 0.1$ for ~10% or $P < 0.2$ for 20% of the control versus DDT sperm or morula comparisons (Supplementary Tables S1–S4 using National Center for Biotechnology Information (NCBI)-provided gene information. Genes were sorted into categories by converting Panther (25) protein classifications into more general groups. A Pathway Studio, Elsevier, database, and network tool was used to assess physiological and disease process gene correlations. For the imprinted genes, rat homologs of previously identified imprinted genes were used and the RPKM read depth for each sample was plotted for the gene location and 50 kb of flanking regions. All molecular data have been deposited into the public database at NCBI (GEO # GSE211135) and R code computational tools are available at GitHub (https://github.com/skinnerlab/MeDIP-seq) and www.skinner.wsu.edu.

Acknowledgements

We acknowledge Dr Rashmi Joshi, Ms Sasha Korolenko, Ms Madelyn Rode, and Mr Grant Rickard for technical assistance. We acknowledge Ms Heather Johnson for her assistance in the preparation of the manuscript. We thank the Genomics Core Laboratory at Washington State University (WSU) Spokane for sequencing data.

Author contributions

Millissia Ben Maamar (Molecular analysis, Data analysis, Manuscript editing), Yue Wang (ICSI morula embryo development, Quality control, Manuscript editing), Eric E. Nilsson (Animal studies, Cell isolations, Data analysis, Manuscript editing), Daniel Beck (Bioinformatic analysis, Data analysis, Manuscript editing), Wei Yan (ICSI embryo oversight, Manuscript editing) and Michael K. Skinner (Conceptualization, oversight, Funding acquisition, Writing, Manuscript editing).

Data availability

All molecular data have been deposited into the public database at NCBI (https://www.ncbi.nlm.nih.gov/geo/) (GEO # GSE211135), and R code computational tools are available at GitHub (https://github.com/skinnerlab/MeDIP-seq and https://skinner.wsu.edu/genomic-data-and-r-code-files/). All computational tools can be uploaded for independent use.

Supplementary data

Supplementary data are available at *EnvEpig* online.

Funding

This study was supported by the John Templeton Foundation (50183 and 61174) (https://templeton.org/) grants to M.K.S. The funders had no role in the study design, data collection and analysis, decision to publish, or preparation of the manuscript.

Conflict of interest statement. The authors have declared that no competing interests exist.

Ethics. All study protocols for the procedures with rats were pre-approved by the Washington State University Animal Care and Use Committee (IACUC approval # 2568 and 6931). All methods were performed in accordance with the relevant guidelines and regulations. This study was carried out in compliance with the ARRIVE guidelines.

References

1. Anway MD, Cupp AS, Uzumcu M *et al.* Epigenetic transgenerational actions of endocrine disruptors and male fertility. *Science* 2005;**308**:1466–9.
2. Franklin TB, Russig H, Weiss IC *et al.* Epigenetic transmission of the impact of early stress across generations. *Biol Psychiatry* 2010;**68**:408–15.
3. Skinner MK, Nilsson EE. Role of environmentally induced epigenetic transgenerational inheritance in evolutionary biology: unified evolution theory. *Environ Epigenet* 2021;**7**:dvab012, 1–12.
4. Jawaid A, Roszkowski M, Mansuy IM. Transgenerational epigenetics of traumatic stress. *Prog Mol Biol Transl Sci* 2018;**158**:273–98.
5. Gapp K, Jawaid A, Sarkies P *et al.* Implication of sperm RNAs in transgenerational inheritance of the effects of early trauma in mice. *Nat Neurosci* 2014;**17**:667–9.
6. Lecoutre S, Kwok KHM, Petrus P *et al.* Epigenetic programming of adipose tissue in the progeny of obese dams. *Curr Genomics* 2019;**20**:428–37.
7. Nilsson E, Sadler-Riggleman I, Skinner MK. Environmentally induced epigenetic transgenerational inheritance of disease. *Environ Epigenet* 2018;**4**:1–13, dvy016.
8. Ben Maamar M, Sadler-Riggleman I, Beck D *et al.* Alterations in sperm DNA methylation, non-coding RNA expression, and histone retention mediate vinclozolin-induced epigenetic transgenerational inheritance of disease. *Environ Epigenet* 2018;**4**:1–19, dvy010.
9. Skinner MK, Ben Maamar M, Sadler-Riggleman I *et al.* Alterations in sperm DNA methylation, non-coding RNA and histone retention associated with DDT-induced epigenetic transgenerational inheritance of disease. *Epigenet Chromatin* 2018;**11**:8, 1–24.
10. Staubli A, Peters AH. Mechanisms of maternal intergenerational epigenetic inheritance. *Curr Opin Genet Dev* 2021;**67**:151–62.
11. Monk M, Boubelik M, Lehnert S. Temporal and regional changes in DNA methylation in the embryonic, extraembryonic and germ cell lineages during mouse embryo development. *Development* 1987;**99**:371–82.
12. Reik W, Surani MA. Germline and pluripotent stem cells. *Cold Spring Harb Perspect Biol* 2015;**7**:a019422, 1–25.
13. Smallwood SA, Kelsey G. Genome-wide analysis of DNA methylation in low cell numbers by reduced representation bisulfite sequencing. *Methods Mol Biol* 2012;**925**:187–97.
14. Farhadova S, Gomez-Velazquez M, Feil R. Stability and lability of parental methylation imprints in development and disease. *Genes (Basel)* 2019;**10**:999, 1–20.
15. Sobocinska J, Molenda S, Machnik M *et al.* KRAB-ZFP transcriptional regulators acting as oncogenes and tumor suppressors: an overview. *Int J Mol Sci* 2021;**22**:2212, 1–26.
16. Sun Y, Keown JR, Black MM *et al.* A dissection of oligomerization by the TRIM28 tripartite motif and the interaction with members of the KRAB-ZFP family. *J Mol Biol* 2019;**431**:2511–27.
17. Monteagudo-Sanchez A, Hernandez Mora JR, Simon C *et al.* The role of ZFP57 and additional KRAB-zinc finger proteins in the maintenance of human imprinted methylation and multi-locus imprinting disturbances. *Nucleic Acids Res* 2020;**48**:11394–407.
18. Zhai Y, Zhang M, An X *et al.* TRIM28 maintains genome imprints and regulates development of porcine SCNT embryos. *Reproduction* 2021;**161**:411–24.
19. Juan AM, Bartolomei MS. Evolving imprinting control regions: KRAB zinc fingers hold the key. *Genes Dev* 2019;**33**:1–3.
20. Jirtle RL, Skinner MK. Environmental epigenomics and disease susceptibility. *Nat Rev Genet* 2007;**8**:253–62.
21. Manikkam M, Tracey R, Guerrero-Bosagna C *et al.* Dioxin (TCDD) induces epigenetic transgenerational inheritance of adult onset disease and sperm epimutations. *PLoS One* 2012;**7**:1–15, e46249.
22. Kubsad D, Nilsson EE, King SE *et al.* Assessment of glyphosate induced epigenetic transgenerational inheritance of pathologies and sperm epimutations: generational toxicology. *Sci Rep* 2019;**9**:6372, 1–17.
23. Tracey R, Manikkam M, Guerrero-Bosagna C *et al.* Hydrocarbons (jet fuel JP-8) induce epigenetic transgenerational inheritance of obesity, reproductive disease and sperm epimutations. *Reprod Toxicol* 2013;**36**:104–16.
24. Manikkam M, Tracey R, Guerrero-Bosagna C *et al.* Pesticide and insect repellent mixture (permethrin and DEET) induces epigenetic transgenerational inheritance of disease and sperm epimutations. *Reprod Toxicol* 2012;**34**:708–19.
25. Manikkam M, Tracey R, Guerrero-Bosagna C *et al.* Plastics derived endocrine disruptors (BPA, DEHP and DBP) induce epigenetic transgenerational inheritance of obesity, reproductive disease and sperm epimutations. *PLoS One* 2013;**8**:1–18, e55387.
26. Manikkam M, Haque MM, Guerrero-Bosagna C *et al.* Pesticide methoxychlor promotes the epigenetic transgenerational inheritance of adult onset disease through the female germline. *PLoS One* 2014;**9**:1–19, e102091.
27. McBirney M, King SE, Pappalardo M *et al.* Atrazine induced epigenetic transgenerational inheritance of disease. Lean phenotype and sperm epimutation pathology biomarkers. *PLoS One* 2017;**12**:1–37, e0184306.
28. Winchester P, Nilsson E, Beck D *et al.* Preterm birth buccal cell epigenetic biomarkers to facilitate preventative medicine. *Sci Rep* 2022;**12**:3361, 1–14.
29. Skinner MK, Manikkam M, Tracey R *et al.* Ancestral dichlorodiphenyltrichloroethane (DDT) exposure promotes epigenetic transgenerational inheritance of obesity. *BMC Med* 2013;**11**:228, 1–16.
30. Han T, Wang F, Song Q *et al.* An epigenetic basis of inbreeding depression in maize. *Sci Adv* 2021;**7**:1–12.
31. Cheptou PO, Donohue K. Epigenetics as a new avenue for the role of inbreeding depression in evolutionary ecology. *Heredity (Edinb)* 2013;**110**:205–6.
32. Pennisi E. European Society for Evolutionary Biology Meeting. Epigenetics linked to inbreeding depression. *Science* 2011;**333**:1563.
33. Skinner MK, Guerrero-Bosagna C. Role of CpG deserts in the epigenetic transgenerational inheritance of differential DNA methylation regions. *BMC Genomics* 2014;**15**:692, 1–6.
34. Beck D, Ben Maamar M, Skinner MK. Genome-wide CpG density and DNA methylation analysis method (MeDIP, RRBS, and WGBS) comparisons. *Epigenetics* 2022;**17**:518–30.
35. Atger V, Wirbel E, Roche D *et al.* Distribution of HDL2 and HDL3 in a random population of healthy French males and females—evaluation by a two-step precipitation procedure. *Clin Chim Acta* 1990;**189**:111–21.
36. Chatterjee A, Rodger EJ, Morison IM *et al.* Tools and strategies for analysis of genome-wide and gene-specific DNA methylation patterns. *Methods Mol Biol* 2017;**1537**:249–77.
37. Nair SS, Coolen MW, Stirzaker C *et al.* Comparison of methyl-DNA immunoprecipitation (MeDIP) and methyl-CpG binding domain (MBD) protein capture for genome-wide DNA methylation analysis reveal CpG sequence coverage bias. *Epigenetics* 2011;**6**:34–44.
38. Toh H, Shirane K, Miura F *et al.* Software updates in the Illumina HiSeq platform affect whole-genome bisulfite sequencing. *BMC Genomics* 2017;**18**:31, 1–8.

39. Nunn A, Otto C, Stadler PF *et al.* Comprehensive benchmarking of software for mapping whole genome bisulfite data: from read alignment to DNA methylation analysis. *Brief Bioinform* 2021;**22**:bbab021, 1–9.
40. Feng S, Jacobsen SE, Reik W. Epigenetic reprogramming in plant and animal development. *Science* 2010;**330**:622–7.
41. Smallwood SA, Tomizawa S, Krueger F *et al.* Dynamic CpG island methylation landscape in oocytes and preimplantation embryos. *Nat Genet* 2011;**43**:811–4.
42. Reik W, Collick A, Norris ML *et al.* Genomic imprinting determines methylation of parental alleles in transgenic mice. *Nature* 1987;**328**:248–51.
43. Surani MA, Allen ND, Barton SC *et al.* Developmental consequences of imprinting of parental chromosomes by DNA methylation. *Philos Trans R Soc Lond B Biol Sci* 1990;**326**: 313–27.
44. Takikawa S, Wang X, Ray C *et al.* Human and mouse ZFP57 proteins are functionally interchangeable in maintaining genomic imprinting at multiple imprinted regions in mouse ES cells. *Epigenetics* 2013;**8**:1268–79.
45. Nilsson E, King SE, McBirney M *et al.* Vinclozolin induced epigenetic transgenerational inheritance of pathologies and sperm epimutation biomarkers for specific diseases. *PLoS One* 2018;**13**:1–29, e0202662.
46. Fitz-James MH, Cavalli G. Molecular mechanisms of transgenerational epigenetic inheritance. *Nat Rev Genet* 2022;**23**:325–41.
47. Olova N, Krueger F, Andrews S *et al.* Comparison of whole-genome bisulfite sequencing library preparation strategies identifies sources of biases affecting DNA methylation data. *Genome Biol* 2018;**19**:33, 1–19.
48. Smallwood SA, Kelsey G. De novo DNA methylation: a germ cell perspective. *Trends Genet* 2012;**28**:33–42.
49. Gomez-Redondo I, Planells B, Canovas S *et al.* Genome-wide DNA methylation dynamics during epigenetic reprogramming in the porcine germline. *Clin Epigenetics* 2021;**13**:27, 1–13.
50. Ben Maamar M, King SE, Nilsson E *et al.* Epigenetic transgenerational inheritance of parent-of-origin allelic transmission of outcross pathology and sperm epimutations. *Dev Biol* 2020;**458**:106–19.
51. Kaneko T, Kimura S, Nakagata N. Offspring derived from oocytes injected with rat sperm, frozen or Freeze-dried without cryoprotection. *Theriogenology* 2007;**68**:1017–21.
52. Huang TT Jr, Yanagimachi R. Inner acrosomal membrane of mammalian spermatozoa: its properties and possible functions in fertilization. *Am J Anat* 1985;**174**:249–68.
53. Calvin HI. Isolation of subfractionation of mammalian sperm heads and tails. *Methods Cell Biol* 1976;**13**:85–104.
54. Bolger AM, Lohse M, Usadel B. Trimmomatic: a flexible trimmer for Illumina sequence data. *Bioinformatics* 2014;**30**:2114–20.
55. Langmead B, Salzberg SL. Fast gapped-read alignment with Bowtie 2. *Nat Methods* 2012;**9**:357–9.
56. Li H, Handsaker B, Wysoker A *et al.* 1000 Genome Project Data Processing Subgroup. The sequence alignment/map format and SAMtools. *Bioinformatics* 2009;**25**:2078–9.
57. Lienhard M, Grimm C, Morkel M *et al.* MEDIPS: genome-wide differential coverage analysis of sequencing data derived from DNA enrichment experiments. *Bioinformatics* 2014;**30**:284–6.
58. Robinson MD, McCarthy DJ, Smyth GK. edgeR: a Bioconductor package for differential expression analysis of digital gene expression data. *Bioinformatics* 2010;**26**:139–40.